Supporting Information for

Rational Design of Electrochemical Sensors Based on Quinone Derivatives Adsorbed on Graphene for the Detection of $[Cd(CN)_4]^{2-}$

Golfer Muedas-Taipe[a], Michael Badawi[b], Angélica María Baena-Moncada[a], and Miguel Ponce-Vargas[b c]**

**email: gmuedast@uni.edu.pe, miguel-armando.ponce-vargas@univ-lorraine.fr*

[a]*Laboratorio de Investigación de Electroquímica Aplicada, Facultad de Ciencias de la Universidad Nacional de Ingeniería, Av. Túpac Amaru 210, Rímac, Lima, Perú.*
[b]*Laboratoire Lorrain de Chimie Moléculaire (L2CM) UMR CNRS 7053, Université de Lorraine. Faculté des Sciences et Techniques, 54500 Vandœuvre-lès-Nancy, France.*
[c]*Université de Reims Champagne-Ardenne, Moulin de la Housse 51687, Reims Cedex 02 BP39, France*

Figure S1. Chronocoulometric results of glassy carbon (GC) electrodes functionalized with quinones **1**, **2**, **3** and **5**, and GC at 0.91 V, t = 60 s in H_2SO_4 0.5 mol L^{-1}.

Figure S2. Limits of detection (LOD) and limits of quantification (LOQ) of glassy carbon (GC) electrodes functionalized with quinones **1**, **2**, **3** and **5**, for the detection of $Na_2[Cd(CN)_4]$ in a 0.1 mol L^{-1} phosphate buffer solution at pH = 5.

Figure S3. Optimized structures of the graphene-ligand systems involving quinones **8**-**14** (**8a**-**14a**) obtained at the M06-2X/6-311G(d) level of theory. The graphene-ligand distances are expressed in Angstroms (Å).

Figure S4. *igmh* analysis of the graphene-ligand systems involving quinones **8**-**14** (**8a**-**14a)**, with an isosurface of 0.01 a.u., and a BGR color code in the range -0.04 a.u. < $\rho\ sign\ (\lambda_2)$ < 0.04 a.u.

Figure S5. *igmh* bonding scores and interaction energies (E_{int}) of systems **8b**-**14b** vs. Hammet parameters of the involved quinone substituents.

Figure S6. Total density of States Analysis (TDOS) of graphene-ligand (**12a**-**14a**) and graphene-complex assemblies (**12b**-**14b**) compared to the TDOS of graphene (gray).

Table S1. *igmh* bonding scores, interaction energies (E_{int}), and Hammet parameters of systems **8b**-**14b**.

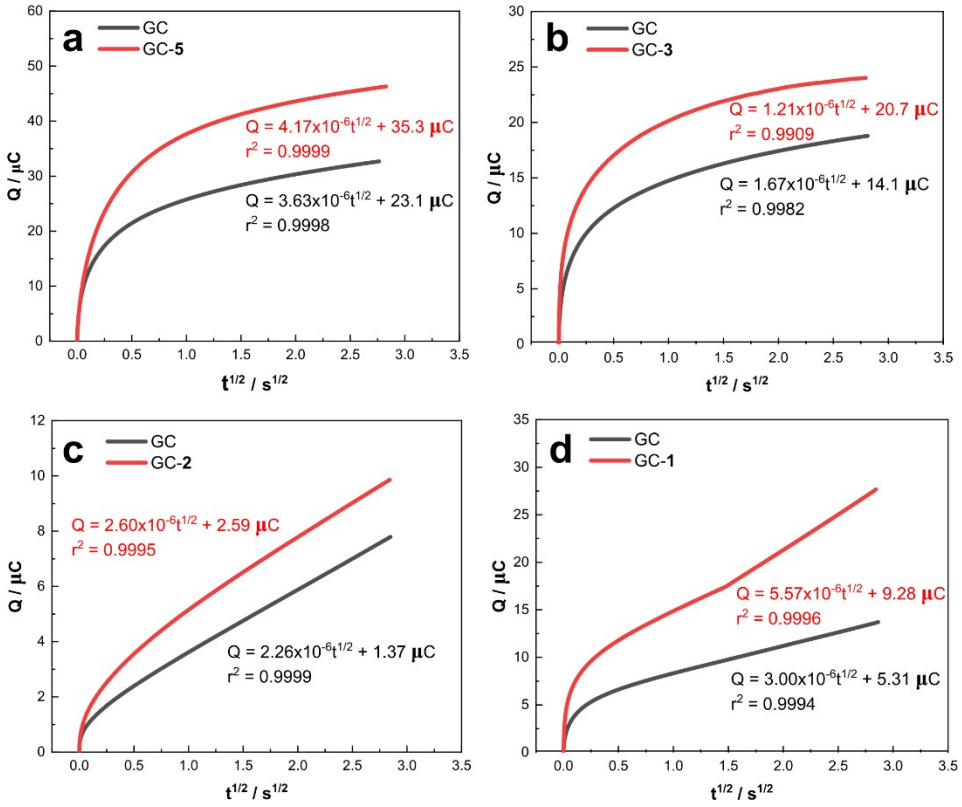

Figure S1. Chronocoulometric results of glassy carbon (GC) electrodes functionalized with quinones **1**, **2**, **3** and **5**, and GC at 0.91 V, t = 60 s in H_2SO_4 0.5 mol L^{-1}.

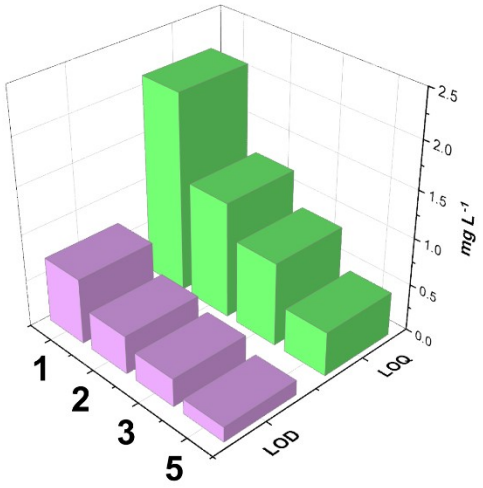

Figure S2. Limits of detection (LOD) and limits of quantification (LOQ) of glassy carbon (GC) electrodes functionalized with quinones **1**, **2**, **3** and **5**, for the detection of $Na_2[Cd(CN)_4]$ in a 0.1 mol L^{-1} phosphate buffer solution at pH = 5.

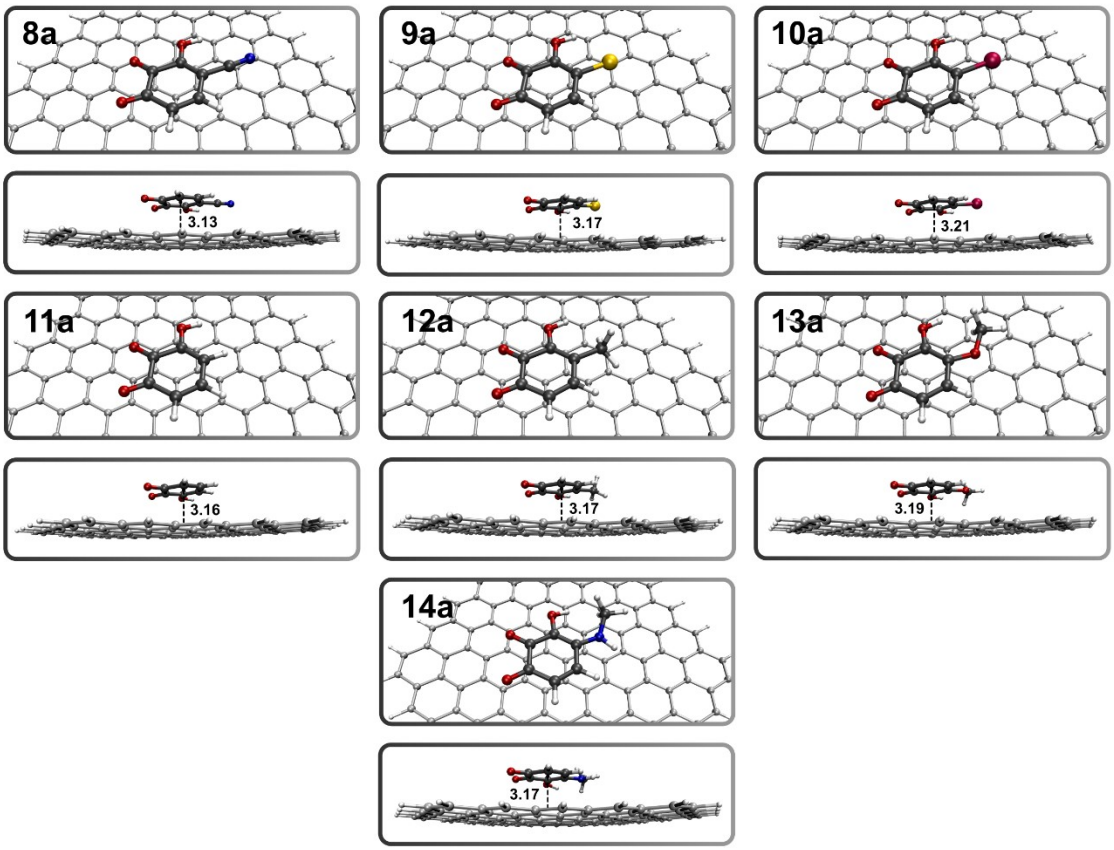

Figure S3. Optimized structures of the graphene-ligand systems involving quinones **8-14** (**8a-14a**) obtained at the M06-2X/6-311G(d) level of theory. The graphene-ligand distances are expressed in Angstroms (Å).

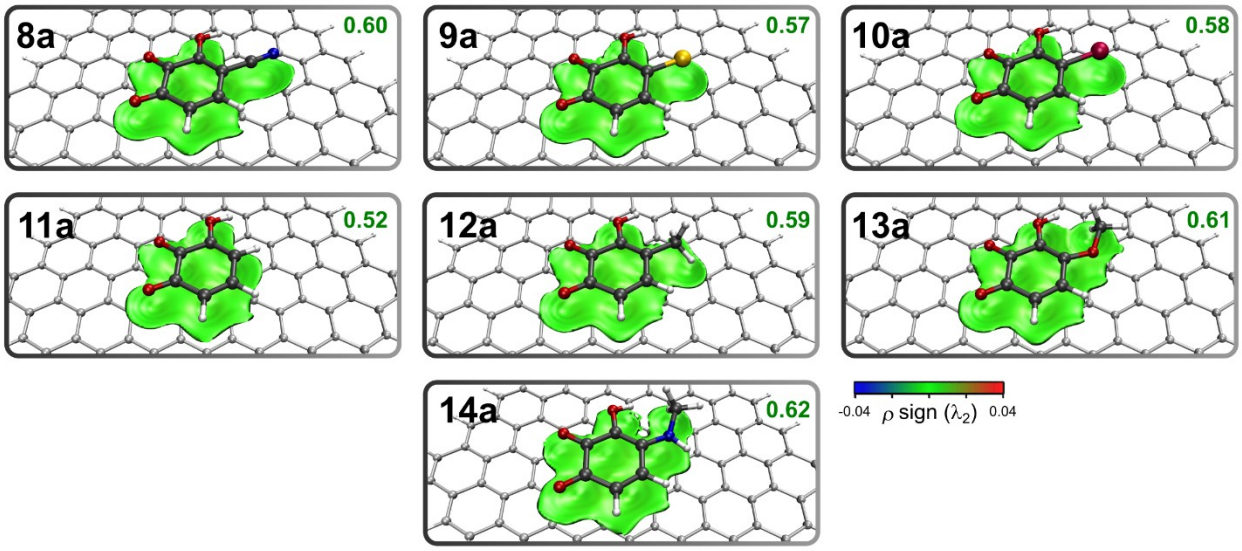

Figure S4. *igmh* analysis of the graphene-ligand systems involving quinones **8-14** (**8a-14a)**, with an isosurface of 0.01 a.u., and a BGR color code in the range -0.04 a.u. < $\rho\ sign\ (\lambda_2)$ < 0.04 a.u.

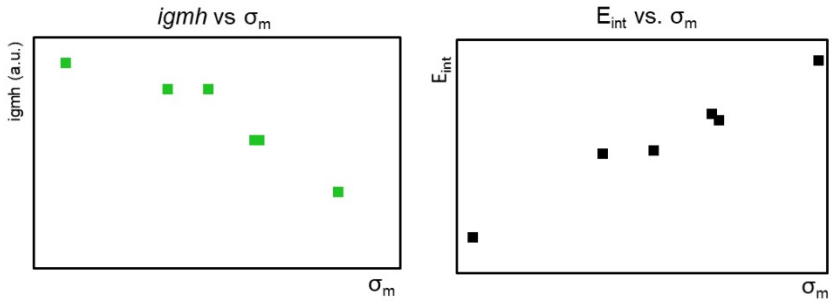

Figure S5. *igmh* bonding scores and interaction energies (E_{int}) of systems **8b**-**14b** vs. Hammet parameters of the involved quinone substituents.

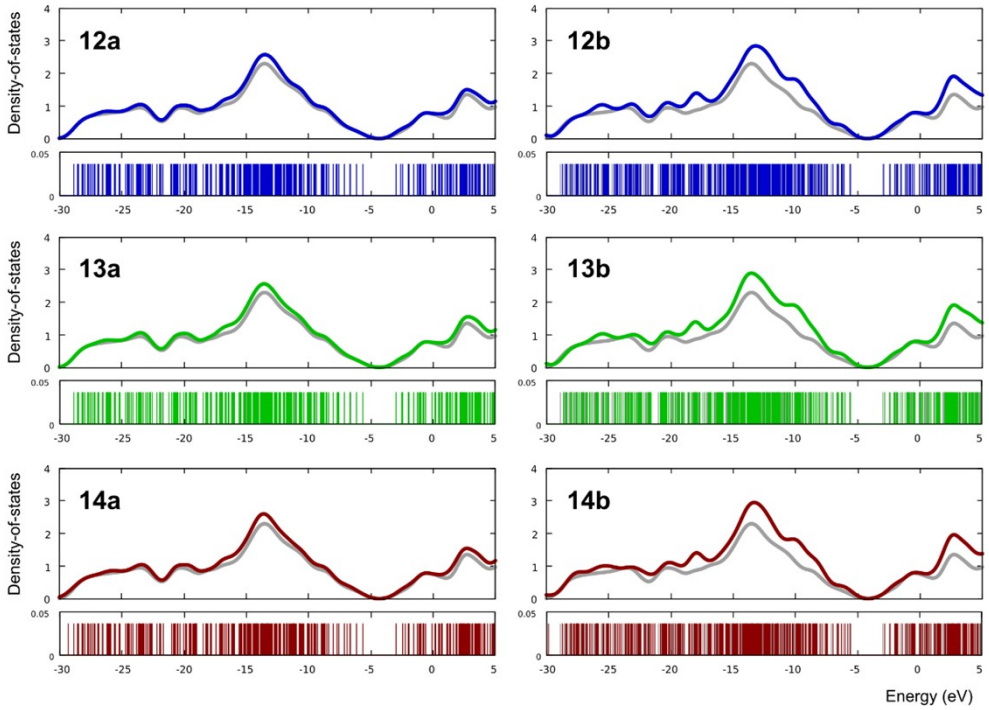

Figure S6. Total density of States Analysis (TDOS) of graphene-ligand (**12a**-**14a**) and graphene-complex assemblies (**12b**-**14b**) compared to the TDOS of graphene (gray).

Table S1. *igmh* bonding scores, interaction energies (E_{int}), and Hammet parameters of systems **8b**-**14b**.

	σ_m	*igmh* (bonding score, a.u.)	E_{int} (complex-graphene, kcal mol^{-1})
-CN	0.66	0.15	-25.6
-Br	0.20	0.17	-27.2
-Cl	0.23	0.17	-27.4
-CH_3	0.05	0.19	-28.3
-OCH_3	0.27	0.19	-28.4
-$NHCH_3$	0.83	0.20	-30.9